J Mater Sci: Mater Med (2011) 22:1205–1211
DOI 10.1007/s10856-011-4310-y

Synthesized silicon-substituted hydroxyapatite coating on titanium substrate by electrochemical deposition

Deng-Hu Li · Jun Lin · Dong-Yang Lin · Xiao-Xiang Wang

Received: 9 October 2010 / Accepted: 25 March 2011 / Published online: 5 April 2011

Abstract Silicon-substituted hydroxyapaptite (Si-HA) coatings were prepared on titanium substrates by electrolytic deposition technique in electrolytes containing Ca^{2+}, PO_4^{3-} and SiO_3^{2-} ions with various $SiO_3^{2-}/(PO_4^{3-} + SiO_3^{2-})$ molar ratios(η_{si}). The deposition was all conducted at a constant voltage of 3.0 V, with titanium substrate as cathode and platinum as anode, for 1 h at 85°C. The coatings thus prepared were characterized with inductively coupled plasma (ICP), X-ray diffraction (XRD), fourier transform infrared spectroscopy (FTIR), field-emission-type scanning electron microscope (FSEM). The results show that the silicon amount in the coatings increases linearly to about 0.48 wt% at first with increasing η_{si} between 0 and 0.03, then increases slowly to about 0.55 wt% between 0.03 and 0.10 and finally maintains almost at a level around 0.55 wt% between 0.10 and 0.30. The tree-like Si-HA crystals are observed in the coatings prepared in the electrolyte of $\eta_{si} = 0.20$. And the presence of silicon in electrolytes decreases the thickness of the coatings, with effect being more significant as η_{si} increased. Additionally, the substitution of Si causes some OH^- loss and changes the lattice parameters of hydroxyapatite (HA).

D.-H. Li · D.-Y. Lin · X.-X. Wang (✉)
Department of Materials Science and Engineering, Zhejiang University, Hangzhou 310027, China
e-mail: msewangxx@zju.edu.cn

J. Lin
The Stomatology Center of the First Affiliated Hospital of Zhejiang University, Hangzhou 310003, China

1 Introduction

Due to its similar chemical composition and crystallographic structure to the inorganic component of bone and tooth [1], synthesized hydroxyapatite (HA) has already been widely used in dentistry and medicine for decades. However, stoichiometric HA has a lower reactivity with natural bone in comparison with bioactive glasses, leading to relative slower rate of osseointegration and, consequently, longer rehabilitation times for the patients [2]. One way that is often used to enhance the bioactive behavior of HA is to obtain substituted apatite that resembles the chemical composition of the mineral phase in bone. Among the various ion substitutions (Na, Mg, Zn, Sr, Zn, Si) that occur at trace (<1 wt%) levels in natural bone [3], silicon is one of the most important trace elements known to be essential in the early stages of bone mineralization and soft tissue development [4]. Actually, in vitro and in vivo studies have already demonstrated that the substitution of phosphate with silicate into HA enhances osteoblast cell activity and has a 14.5% increase in bone in-growth versus HA controls [5, 6]. And, silicon-substituted hydroxyapatite (Si-HA) has already been prepared with many different methods in powder form by researchers all over the world, such as sol–gel, hydrothermal, solid-state reaction, aqueous precipitation and controlled crystallization.

On the other hand, HA coating is one of the most important applications of HA material. Considering the advantage of Si-HA powder, Si-HA coating is expected to have better bioactivity than HA coating. Nowadays, a number of coating techniques, including plasma spray [7], biomimetic [8], magnetron co-sputtering [9], sol–gel [10] and pulse laser deposition [11], have been developed to prepare Si-HA coating. The coating technique of electrolytic deposition has attracted considerable attention

recently, because of its low temperature and cost, the control of coating thickness and chemical composition, and the ability to coat irregular implant surface [12–14]. In our laboratory, Jiao et al. [15] have synthesized magnesium-substituted HA coatings successfully on titanium surface using electrolytic deposition. So far, Si-HA coating deposited by this technique has not been reported. In this work, we tried the possibility of preparing Si-substituted HA coatings by electrochemical deposition on titanium substrates.

2 Materials and methods

2.1 Materials

The commercially pure titanium (CP Ti) plates in dimension of 10 × 10 × 1 mm were used as substrate for coating. Their surfaces were mechanically ground on SiC papers from P400 to P800, etched in an acid mixture ($HF:HNO_3:H_2O$ = 1:3:10), ultrasonicated in acetone and then rinsed with deionized water.

2.2 Electrodeposition

Electrolytes for HA deposition were prepared by dissolving given amounts of reagent-grade chemicals: $CaCl_2$, $NH_4H_2PO_4$, NaCl and $Na_2SiO_3{\cdot}9H_2O$ in deionized water, with $Na_2SiO_3{\cdot}9H_2O$ served as silicon source and NaCl (0.1 M/L) as conductive agent. The concentrations of Ca^{2+} and (PO_4^{3-} + SiO_3^{2-}) in all electrolytes were kept at 1.2 and 0.72 mM, respectively, with various SiO_3^{2-}/(PO_4^{3-} + SiO_3^{2-}) molar ratios in electrolytes (η_{Si}) of 0, 0.01, 0.02, 0.03, 0.04, 0.05,0.10, 0.20 and 0.30, assuming that the silicate ions would substitute the phosphate ions. The pH was adjusted to 6.0 by addition of hydrochloric acid and ammonia at room temperature. The electrochemical process was carried out with a potentiostat (CHI1140, USA) at a settled voltage of 3.0 V for 1 h with Ti substrate used as the working electrode (cathode) and platinum (Pt) plate as the counter electrode (anode) at temperature of 85°C.

2.3 Characterization

The coatings were dissolved in 50 ml of 0.1 M HCl and the concentrations of Ca, P and Si in solutions were measured by inductively coupled plasma-atomic emission spectrometry (ICP-AES, IRIS IntrepidII, XPS type ICP-AES,AEP Co.Inc). The concentration of Ca was used to calculate the total weight of each coating, supposing that the deposit is stoichiometrical HA, and the concentrations of Si and P were used to calculate the weight percent and molar percent of silicon in the coatings.

The surface morphology was observed with a field-emission-type scanning electron microscope (FESM, Hitachi S4800). The crystal phase of the deposit was examined using an X-ray diffractometer (XRD, X-Pert Pro) with Cu Kα radiation. The crystal structural parameters of HA along with Si-HA deposited in the electrolyte of η_{si} = 0.20 were calculated by Rietveld refinement of the X-ray diffraction data, and the refinements were based on the structural data of Kay et al. [16] using the space group *P*63/m. In order to acquire high quality XRD spectra, data were collected with a step size of 0.017° and a count rate of 0.025°/min for the use of Rietveld refinement. Spectroscopic analysis of the deposit powder was carried out with fourier transform infrared spectroscopy (FT-IR AVATAR) using KBr pellet technique. With the help of stylus profiler (Dektak 3, Veeco), the coating thickness was determined.

3 Results and discussion

3.1 The composition of the coatings

The variation of silicon amount in the coatings with different η_{si} is shown in Fig. 1. It can be seen that the weight percent of silicon in the coatings increases sharply to 0.48 wt% with increasing η_{si} when η_{si} <0.03, then increases slowly when η_{si} = 0.03–0.10, and finally maintains almost at around 0.55 wt% when η_{si} = 0.10–0.30. The molar percent of silicon (Si/(Si + P) molar ratio) in the coatings follows the similar trend of the weight percent of silicon versus η_{si} when η_{si} ≤0.20, but obviously deviates from the trend for the electrolyte of η_{si} = 0.30. The results confirm that the electrochemical deposition is a controllable method to prepare Si-HA coatings on Ti substrates. The approximate linear relationship both for weight and molar

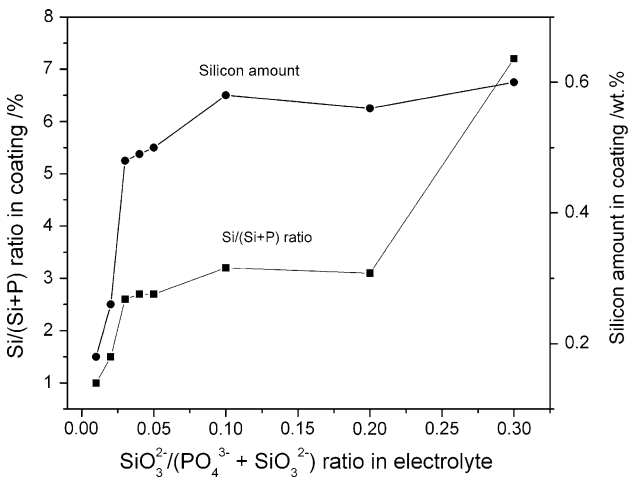

Fig. 1 The measured wt% of silicon and Si/(Si + P) molar ratio in coatings versus SiO_3^{2-}/(PO_4^{3-} + SiO_3^{2-}) molar ratio in electrolytes

percent of silicon in the coatings at η_{si} <0.03 indicates that silicon can be incorporated into coatings proportionally to η_{si}. But the situation is different in the range of η_{si} from 0.03 to 0.30 where the silicon concentration in the coatings increases slowly to a saturation value of 0.55 wt% and then levels off. Interestingly, the silicon molar percent in coatings prepared in electrolyte of $\eta_{si} = 0.30$ deviates substantially from the trend, which may correlate with the formation of calcium phosphate phases other than HA (e.g. amorphous calcium phosphate) in the coatings.

The limited silicon amount in electrochemically deposited coatings may be dominatingly attributed to the greater radius of Si^{4+} compared with P^{5+} and thus higher obstacle energy for silicon ions entering the HA lattice. Vallet-Regí et al. [17] have pointed out that silicon is mainly incorporated during the subsequent thermal treatment after the formation of calcium phosphate phases from aqueous solution in Si-HA precipitation process. The Si-HA powders [20] and coatings [10] with silicon content more than 1 wt% have been reported prepared with high temperature treatment in hydrothermal method and sol–gel method, respectively. Obviously, the temperature of 85°C in present electrolytic deposition cannot provide enough energy for silicon incorporation. Moreover, the electrostatic repulsion between silicate ions and substrate may dilute the silicon concentration in the solution around the substrate, and, consequently, affect the silicon amount in the coatings. Zhang et al. [8] have shown that Si-HA coating on porous Ti with 0.39 wt% silicon exhibited significantly higher bioactivity than HA coating at the same condition. Other studies have also reported that silicon content in natural bone reached a level of 0.5 wt% in active calcification sites [4]. Thus, the silicon amount of around 0.55 wt% in the coatings may be enough to yield substantial bioactive improvements.

3.2 XRD and FTIR characterization of the coatings

The XRD patterns of as-prepared coatings were obtained and are shown in Fig. 2. The patterns of all coatings exhibit characteristic diffractions of HA, suggesting that the main crystal phase of coatings is HA. And, the HA crystals in all coatings are preferentially oriented with [001] direction perpendicular to Ti substrate, as evidenced by the substantially stronger relative intensity of (002) diffraction compared to the standard HA diffraction pattern. With increasing η_{si}, the intensity of the HA diffractions is gradually decreased. This may be attributed to the decreasing total mass of the coatings deposited on Ti substrates, and probably, especially for the case of $\eta_{si} = 0.20$ (Fig. 2d), the presence of amorphous calcium phosphate or calcium phosphate phases other than HA. Unfortunately, the low mass quantity of Si-HA coatings deposited on Ti substrates in electrolytes of $\eta_{si} \geq 0.20$ makes the detection of impurity phases difficult.

FTIR was used to qualify the effect of the silicon substitution on the different functional groups of HA coatings. As shown in Fig. 3, typical absorption bands from three ionic groups of HA are observed: the bands at 3,570 and 630 cm^{-1} correspond to the stretching and bending modes of O–H, respectively, the bands at 1,089, 1,038 and 962 cm^{-1} are assigned to P–O stretching modes, the bands at 603 and 507 cm^{-1} are associated with O–P–O bending modes, and finally the bands at 1,456, 1,410 and 875 cm^{-1} of carbonate groups can be detected in all coatings, probably due to the

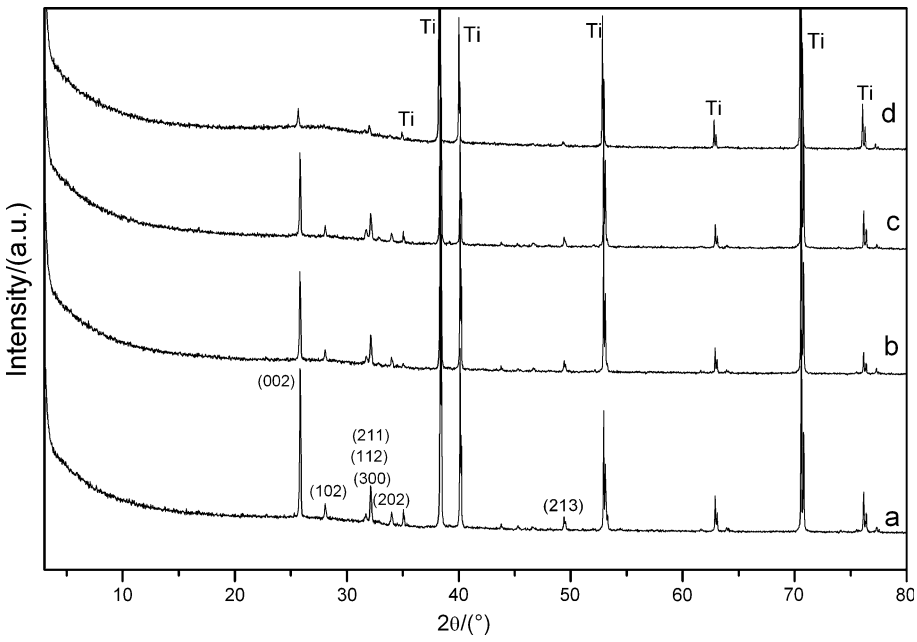

Fig. 2 XRD patterns of the coatings deposited on titanium in the electrolytes with various $SiO_3^{2-}/(PO_4^{3-} + SiO_3^{2-})$ molar ratio: (*a*) 0, (*b*) 0.05, (*c*) 0.10, (*d*) 0.20

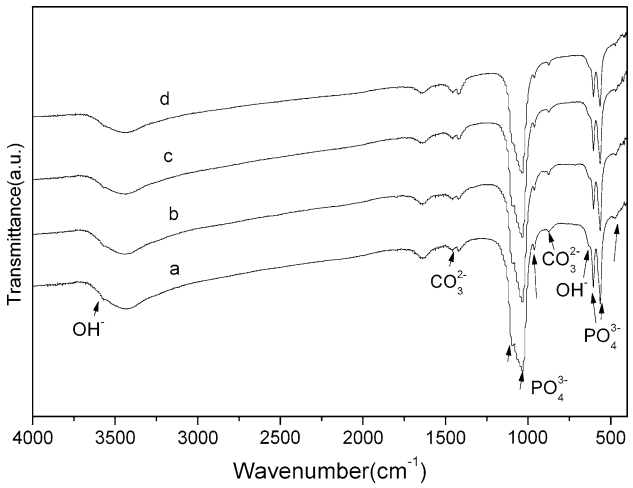

Fig. 3 FTIR spectra of deposits scraped from the titanium surface prepared in electrolytes with various $SiO_3^{2-}/(PO_4^{3-} + SiO_3^{2-})$ molar ratio: (*a*) 0, (*b*) 0.05, (*c*) 0.10, (*d*) 0.20

absorption of CO_2 from the air [18]. Compared with the FTIR spectra of the HA, PO_4 bands at 1,089, 1,038 cm^{-1} seem to be merged after silicon incorporation and the PO_4 bands at 962, 470 cm^{-1} are all decreased with increasing silicon incorporation, suggesting that the silicate tetrahedra are substituted for the phosphate tetrahedra in the HA structure. The OH absorption bands at 3,570 and 630 cm^{-1} are also decreased slightly with increasing silicon incorporation. And some of obvious silicate absorption bands are not detected in FTIR spectra, possibly due to the limited amount of silicate and the stronger overlapping absorption bands from HA. The main SiO_4 bands are located at 1,185, 1,085–1,000, 890, 870 and 840 cm^{-1} [19–21] where carbonated HA happens to have various vibration bands.

Although the first additive used as silicon source in electrolytes is SiO_3^{2-}, silicon ions may be incorporated into HA in the form SiO_4^{4-} rather than SiO_3^{2-}. This could be corroborated by the decreased OH^- groups in HA, as evidenced in the FTIR spectra and that is required by the charge balance during the substitution of PO_4^{3-} with SiO_4^{4-} [20–22]. At pH value of 6, the SiO_3^{2-} may have reactions in aqueous solution as follows [23]:

$$H_2O + SiO_3^{2-} \rightarrow H_2SiO_4^{2-} \quad (1)$$

$$H_2SiO_4^{2-} \rightarrow H^+ + HSiO_4^{3-} \quad (2)$$

$$HSiO_4^{3-} \rightarrow H^+ + SiO_4^{4-} \quad (3)$$

When a voltage is applied, cathodic reactions (4)–(7) occur during the deposition process [24]:

$$2H^+ + 2e^- \rightarrow H_2 \quad (4)$$

$$2H_2O + 2e^- \rightarrow H_2 + 2OH^- \quad (5)$$

$$H_2PO_4^- + OH^- \rightarrow H_2O + HPO_4^{2-} \quad (6)$$

$$HPO_4^{2-} + OH^- \rightarrow H_2O + PO_4^{3-} \quad (7)$$

Reactions (1)–(3) transform SiO_3^{2-} to SiO_4^{4-} in solution. Reactions(4)–(5) yield OH^- ions which increase the pH and the degree of supersaturation relative to HA at the vicinity of titanium substrate [24]. Reactions (6)–(7) yield PO_4^{3-} ions. As a result, Si-HA crystals are deposited on Ti substrates through the following reaction:

$$10Ca^{2+} + (6-x)PO_4^{3-} + xSiO_4^{4-} + (2-x)OH^- \rightarrow Ca_{10}(PO_4)_{6-x}(SiO_4)_x(OH)_{2-x} \quad (8)$$

3.3 Thickness measurement and the lattice parameters

The thickness and the total mass of the coatings are plotted against the η_{si} in Fig. 4. The pure HA coating reaches to 3.5 μm in thickness. As silicon is added in the electrolytes, the thickness of Si-HA coating decreases from 2 μm at $\eta_{si} = 0.05$–1.4 μm at $\eta_{si} = 0.10$, and further to 0.7 μm at $\eta_{si} = 0.20$. In most Si-HA preparation methods, both for powders and coatings, the presence of silicon tends to inhibit grain growth. It is also true for the electrolytically deposited Si-HA coating. The gradually decreased thickness with increasing η_{si} clearly demonstrates that the presence of silicon in electrolyte inhibits the Si-HA crystal growth. Meanwhile, the total mass of the coatings shows the same trend with thickness change. These results are consistent with XRD result. Furthermore, the change of the coating thickness cannot be the effect of the decreasing PO_4^{3-} concentration in electrolytes, as the same thickness is observed in the coatings obtained in electrolytes of reducing PO_4^{3-} ions without silicon addition, and still many ions are remained in the electrolyte.

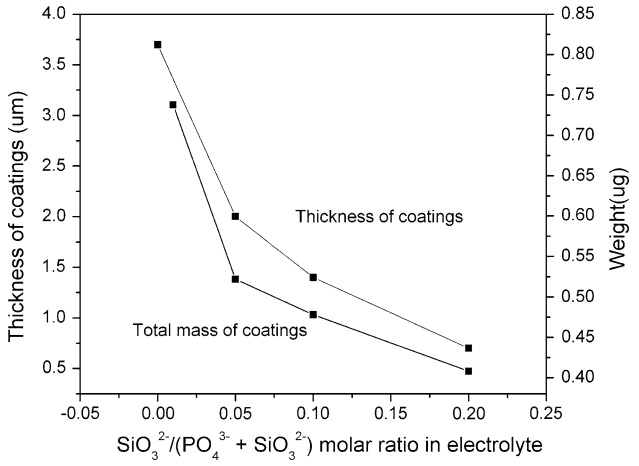

Fig. 4 The thickness and total mass change of coatings prepared with different $SiO_3^{2-}/(PO_4^{3-} + SiO_3^{2-})$ molar ratio in electrolytes

Table 1 Lattice parameters of HA and Si-HA coatings

Sample	a/nm	c/nm	Unit cell volume/nm^3
HA	0.94344	0.68815	0.52997
Si-HA($\eta_{si} = 0.2$)	0.94303	0.68969	0.52995

The lattice parameters and unit cell volume of the Si-HA were calculated from Rietveld structure of the X-ray diffraction data, which are shown in Table 1. The substitution of silicon results in a slight decrease in the a-axis and increase in the c-axis of the HA unit cell, although the actual unit cell volume remains almost unchanged. These small changes in the crystal structure of HA may be attributed to the incorporation of larger silicon ions and the loss of some OH ions in the crystal structure.

Obviously, silicon is incorporated into HA lattice in the coatings as demonstrated by FTIR and the change of HA lattice parameters. Once silicon exists in HA lattice, it will cause HA crystals to be more soluble in aqueous solution and to release more Ca^{2+} and PO_4^{3+} ions into the culture medium [25], thus forming a new apatite layer on substrate more quickly which provides an ideal site for the cells to attach, proliferate and form new bone [26]. With trace silicate being in the culture medium, it will form a bound silicate network structure on the coating surface which has been shown to have the capability of bonding proteins together in an organized manner [27], and in turn to promote better cell attachment via an interaction with the integrin on the human osteoblast cells.

3.4 Surface characterization

Figure 5 shows the crystal morphology of Si-HA coatings formed in electrolytes of various η_{si}. As revealed by SEM, rod-like crystals with a hexagonal cross section and diameters of about 100 nm are observed in the pure HA coating. And almost the same morphology is observed in the Si-HA coatings obtained in electrolytes of $\eta_{si} = 0.05$ and 0.10, except that these Si-HA crystals are denser and more compact compared to pure HA crystals. Increase in η_{si} to 0.20 results in the appearance of tree-like crystals (Fig. 5d) in the coatings whose branches keep the same hexagonal morphology.

The early growth stages of the tree-like crystals are shown in Fig. 6. As can be seen, the plate-like precursor is firstly deposited on Ti substrate, then converts to rod-like crystals after continuous electrochemical deposition process. Several rod-like crystals are able to be transformed simultaneously from one plate-like precursor during the process of conversion, forming a bundle of rod crystals (Fig. 6c). Due to their slow rate of growth, particularly in [001] direction, the crystal morphology in Fig. 5d is obtained. Nevertheless, the growth in [100] direction is not inhibited significantly, leaving the characteristic hexagonal cross section of HA crystals unchanged after 1 h deposition. Another possible explanation is that the substitution of more negatively charged silicate ions for phosphate ions may occur on (100) prism surfaces on which the PO_4^{3-} anions are usually exposed. As a consequence, the (100) prism surfaces become more negative charged, and thus may facilitate the secondary

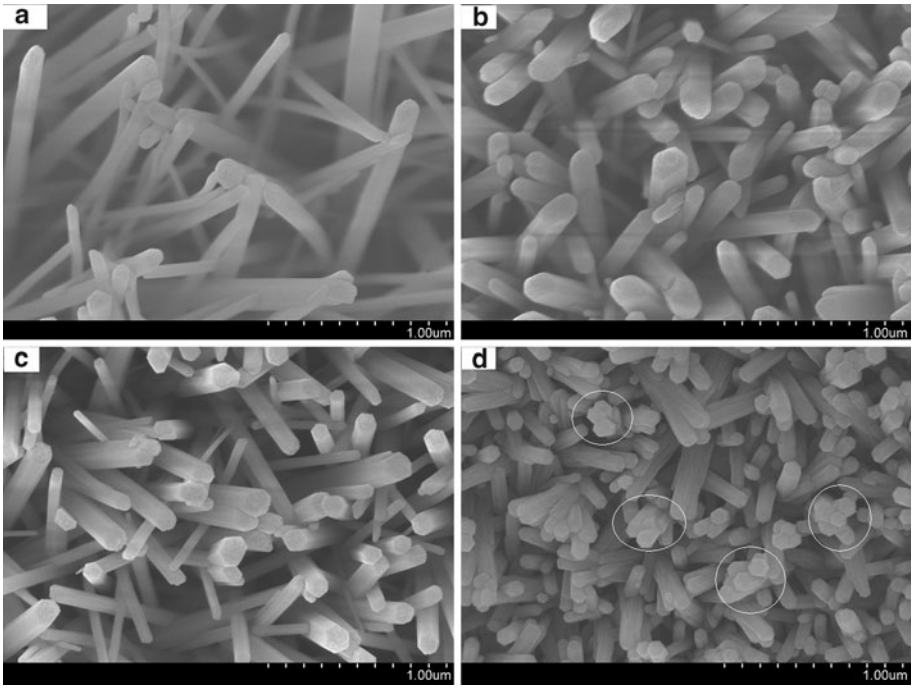

Fig. 5 SEM images of the coatings prepared in electrolytes with various $SiO_3^{2-}/(PO_4^{3-} + SiO_3^{2-})$ molar ratio: **a** 0, **b** 0.05, **c** 0.10, **d** 0.20

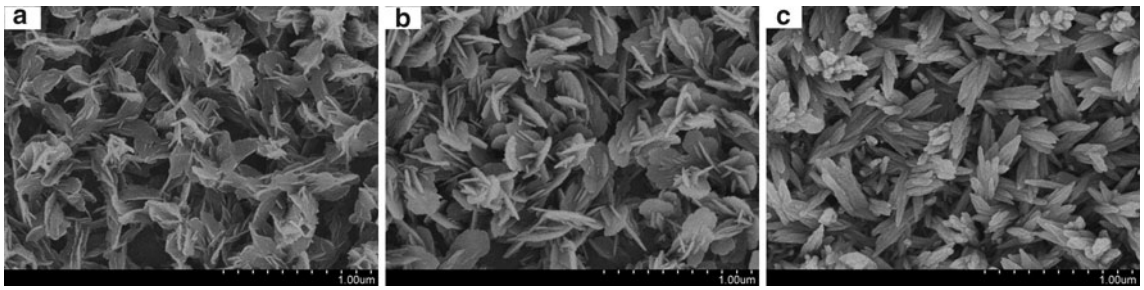

Fig. 6 SEM images of the tree-like crystals in early stages time in electrolyte with $SiO_3^{2-}/(PO_4^{3-} + SiO_3^{2-})$ molar ratio being 0.20: **a** 8 min, **b** 10 min, **c** 12 min

nuclei on the (100) surfaces [28]. Thian et al. [29] have already demonstrated that it is the modification of the surface wettability and increased surface charge by the substitution of silicon into the HA crystal lattice, that enhance the early stage protein expression on the Si-HA surface.

4 Conclusions

Using electrolytic deposition, uniform Si-HA phase coatings with 0.7–1.4 μm in thickness were successfully prepared on Ti substrates. The weight percent of silicon in the coatings increases linearly to about 0.48 wt% at first with increasing η_{si} between 0 and 0.03, then increases slowly to about 0.55 wt% between 0.03 and 0.10 and finally maintains almost at a level around 0.55 wt% between 0.10 and 0.30. The presence of silicon in electrolyte plays an inhibiting role in the growth of Si-HA crystals, leading to the decreasing of coating thickness and the formation of tree-like Si-HA crystals in the electrolyte of $\eta_{si} = 0.20$. The substitution of silicon results in loss of some OH^- ions which is associated with charge balance, and causes some minor changes of HA crystal structure.

Acknowledgment This study was financially supported by National Natural Science Foundation of China (NSFC) under the grant number 50571088.

References

1. Suchanek W, Yoshimura M. Processing and properties of hydroxyapatite-based biomaterials for use as hard tissue replacement implants. J Mater Res. 1998;13:94–117.
2. Höland W, Vogel W, Naumann K, Gummel J. Interface reactions between machinable bioactive glass-ceramics and bone. J Biomed Mater Res. 1985;19:303–12.
3. Elliot J. Structure and chemistry of the apatites and other calcium orthophosphates. Amsterdam: Elsevier; 1994.
4. Carlisle EM. Silicon: a possible factor in bone calcification. Science. 1970;167:279–80.
5. Gibson I, Hing JA, Best S, Bonfield W. Enhanced in vitro cell activity and surface apatite layer formation on novel silicon-substituted hydroxyapatites. Bioceramics. 1999;12:191–4.
6. Patel N, Best S, Bonfield W, Gibson I, Hing K, Damien E, Revell P. A comparitive study on the in vivo behavior of hydroxyapatite and silicon substituted hydroxyapatite granules. J Mater Sci Mater Med. 2002;13:1199–206.
7. Tang Q, Brooks R, Rushton N, Best M. Production and characterization of HA and SiHA coatings. J Mater Sci Mater Med. 2010;21:173–81.
8. Zhang E, Zou C. Porous titanium and silicon-substituted hydroxyapatite biomodification prepared by a biomimetic process: characterization and in vivo evaluation. Acta Biomater. 2009;5:1732–41.
9. Thian E, Huang J, Vickers M, Best S, Barber Z, Bonfield W. Silicon-substituted hydroxyapatite (Si-HA): a novel calcium phosphate coating for biomedical applications. J Mater Sci. 2006;41:709–17.
10. Hijon N, Cabanas M, Pena J, Vallet-Regi M. Dip coated silicon-substituted hydroxyapatite films. Acta Biomater. 2006;2:567–74.
11. Yang Y, Paital SR, Dahotre NB. Effects of SiO_2 substitution on wettability of laser deposited Ca-P biocoating on Ti-6Al-4V. J Mater Sci Mater Med. 2010;21:2511–21.
12. Ban S, Maruno S. Effect of temperature on electrochemical deposition of calcium phosphate coatings in a simulated body fluid. Biomaterials. 1995;16:977–81.
13. Ye W, Wang XX. Ribbon-like and rod-like hydroxyapatite crystals deposited on titanium surface with electrochemical method. Mater Lett. 2007;61:4060–5.
14. Ma M, Ye W, Wang XX. Effect of supersaturation on the morphology of hydroxyapatite crystals deposited by electrochemical deposition on titanium. Mater Lett. 2008;62:3875–7.
15. Jiao MJ, Wang XX. Electrolytic deposition of magnesium-substituted hydroxyapatite crystals on titanium substrate. Mater Lett. 2009;63:2286–9.
16. Kay MI, Young RA, Posner AS. A crystal structure of hydroxyapatite. Nature. 1964;204:1050–2.
17. Vallet-Regí M, Arcos D. Silicon substituted hydroxyapatite. A method to upgrade calcium phosphate based implants. J Mater Chem. 2005;15:1509–16.
18. Rößler S, Sewing A, Stölzel M, Scharnweber M, Dard M, Worch H. Electrochemically assisted deposition of thin calcium phosphate coatings at near-physiological pH and temperature. J Biomed Mater Res. 2002;64:655–63.
19. Andersson J, Areva S, Spliethoff B, Lindén M. Sol–gel synthesis of a multifunctional, hierarchically porous silica/apatite composite. Biomaterials. 2005;26:6827–35.
20. Leventouri T, Bunaciu C, Perdikatsis V. Neutron powder diffraction studies of silicon-substituted hydroxyapatite. Biomaterials. 2004;24:4205–21.
21. Gibson I, Best S, Bonfield W. Chemical characterization of silicon-substituted hydroxyapatite. J Biomed Mater Res. 1999;44:422–8.

22. Tang X, Xiao X, Liu R. Structural characterization of silicon-substituted hydroxyapatite synthesized by hydrothermal method. Mater Lett. 2005;59:3841–6.
23. Zhang E, Zou C, Zeng S. Preparation and characterization of silicon-substituted hydroxyapatite coating by a biomimetic process on titanium substrate. Surf Coat Technol. 2009;23:1075–80.
24. Lin DY, Wang XX. Electrodeposition of hydroxyapatite coating on CoNiCrMo substrate in dilute solution. Surf Coat Technol. 2010;204:3205–13.
25. Porter AE, Patel N, Skeeper JN, Best SM, Bonfield W. Comparison of in vivo dissolution processes in hydroxyapatite and silicon-substituted hydroxyapatite ceramics. Biomaterials. 2003;24:4609–20.
26. Thian E, Huang J, Best S, Barber Z, Brooks R, Rushton N, Bonfield W. The response of osteoblasts to nanocrystalline silicon-substituted hydroxyapatite thin films. Biomaterials. 2005;27:2692–8.
27. Thian E, Huang J, Best S, Barber Z, Bonfield W. Silicon-substituted hydroxyapatite: the next generation of bioactive coatings. Mater Sci Eng C. 2007;27:251–6.
28. Chen X, Wu T, Wang Q, Shen JW. Shield effect of silicate on adsorption of proteins onto silicon-doped hydroxyapatite (100) surface. Biomaterials. 2008;29:2423–32.
29. Thian ES, Ahmad Z, Huang J, Edirisinghe MJ, Jayasinghe SN, Ireland DC, Brooks RA, Rushton N, Bonfield W, Best SM. The role of surface wettability and surface charge of electrosprayed nanoapatites on the behavior of osteoblasts. Acta Biomater. 2010;6:750–5.